Observation and Modelling of Fast Ion Loss

S. D. Pinches[1], V. G. Kiptily[2], S. E. Sharapov[2], D. S. Darrow[3],

L.-G. Eriksson[4], H.-U. Fahrbach[1], M. García-Muñoz[1], M. Reich[1], E. Strumberger[1],

A. Werner[1], the ASDEX Upgrade Team and JET-EFDA Contributors[†]

[1]*Max-Planck Institut für Plasmaphysik, EURATOM-Assoziation, Boltzmannstraße 2, D-85748 Garching, Germany*
[2]*EURATOM/UKAEA Fusion Association, Culham Science Centre, OX14 3DB, UK*
[3]*Princeton Plasma Physics Laboratory, P.O. Box 451, Princeton, New Jersey 08543, USA*
[4]*Association EURATOM-CEA, CEA-Cadarache, F-13108 St. Paul lez Durance, France*

Email: Simon.Pinches@ipp.mpg.de

Abstract

The confinement of fast particles is of crucial importance for the success of future burning plasma experiments.. On JET, the confinement of ICRF accelerated fast hydrogen ions with energies exceeding 5 MeV has been measured using the characteristic γ-rays emitted through their inelastic scattering with carbon impurities, $^{12}C(p,p'\gamma)^{12}C$. Recent experiments have shown a significant decrease in this γ-ray emission (by a factor of 2) during so-called tornado mode activity (core-localised TAEs within the q = 1 surface) in sawtoothing plasmas. This is indicative of a significant loss or extensive re-distribution of these (> 5 MeV) particles from the plasma core. In this paper, mechanisms responsible for the radial transport and loss of these fast ions are investigated and identified using the HAGIS code, which describes the interaction of the fast ions and the TAE observed. The calculations show that the overlap of wave-particle resonances in phase-space leads to an enhanced radial transport and loss. On both JET and ASDEX Upgrade, new fast ion loss detectors have been installed to further investigate the loss of such particles. On JET, fast ion loss detectors based around an array of Faraday cups and a scintillator probe have been installed as part of a suite of diagnostic enhancements. On ASDEX Upgrade, a new fast ion loss detector has been mounted on the mid-plane manipulator allowing high resolution measurements in pitch angle, energy and time. This has enabled the direct observation of fast ion losses during various MHD phenomena to be studied in detail. ELM induced fast ion losses have been directly observed along with the enhancement of fast ion losses from specific areas of phase-space in the presence of NTMs and TAEs.

Introduction and Overview

The success of magnetically confined fusion plasmas relies upon the satisfactory confinement of the energetic fusion products for sufficiently long that the fuel ions are heated by them to a level where they start to fuse and a self-sustained burn process is achieved [1]. Furthermore, losses of these energetic ions can only be tolerated at very low levels to prevent damage to the vessel first wall.

New fast ion loss diagnostics have now been installed on both ASDEX Upgrade [15] and JET [2,3] to measure the distribution of lost fast ions. In addition to starting to address technology issues associated with the detection of fast ion loss in an ITER-relevant environment (e.g. high neutron flux and thermal load), they are also already providing valuable information that can be used to benchmark and further develop numerical codes capable of simulating such losses.

[†] See the Appendix of J. Paméla et al., Fusion Energy 2004 (Proc. 20th Int. Conf. Vilamoura, 2004) IAEA, Vienna (2004)

There are predicted to be two primary single particle loss mechanisms for α-particles in a future reactor, both of which can be related to imperfections in the confining magnetic field structure. The first arises from the use of a finite number of toroidal field coils to generate the strong toroidal magnetic field leading to a ripple in field strength. The orbits of ripple trapped banana particles are not closed and their turning points experience a small, but finite vertical displacement after each bounce. When the vertical excursions of the banana-tips exceed a certain threshold, stochasticity occurs, leading to a diffusion-like phenomenon [4]. The resulting diffusion coefficient depends both on the ripple magnitude, $\delta \equiv (B_{max} - B_{min})/(B_{max} + B_{min})$ and the particle energy. When the ripple is important, particles are lost within a few hundred bounces; a time much shorter than their slowing down time.

The other type of magnetic field imperfection that can lead to fast ion losses are self-generated and arise from plasma instabilities. This category includes the Toroidal Alfvén Eigenmode (TAE) which is a shear Alfvén wave that can resonantly interact with fast ions that have speeds close to the Alfvén speed leading to their redistribution and even loss. Core-localised TAE (CL-TAE) [5] which exist in the low magnetic shear region near the centre of the plasma ("tornado modes" are CL-TAE within the $q = 1$ surface [6]) have been observed on JET to lead to an extensive re-distribution of the fast ion population. The observation and modelling of this process forms the topic of the next section where in addition to the two mechanisms outlined above, fast particles are also lost because they are born on unconfined orbits. These particles are referred to as prompt loss particles and the effect of the tornado modes is to lead to an enhancement of these losses.

Experimental Observations and Modelling of Fast Ion Loss on JET

Observations made with the vertical γ-ray spectrometer [7] mounted on JET have revealed a significant decrease (by a factor of 2) in the γ-rays born as a result of inelastic scattering between ICRF accelerated hydrogen minority ions (fast protons) and carbon impurities in the plasma, $^{12}C(p,p'\gamma)^{12}C$, during so-called "tornado mode" activity (CL-TAE within the $q = 1$ surface) [8]. This reduction in characteristic γ-ray emission is indicative of a loss or extensive re-distribution of these (> 5 MeV) ions. In this section, the mechanism behind the re-distribution and loss of these fast ions is elucidated. The focus of the study is an identification of whether such losses arise due to a resonant wave-particle interaction, or whether they are simply due to a modification of the prompt loss boundaries due to the distortion of the flux surfaces arising from the AE present. Losses in this latter category would be expected to scale linearly with the AE amplitude.

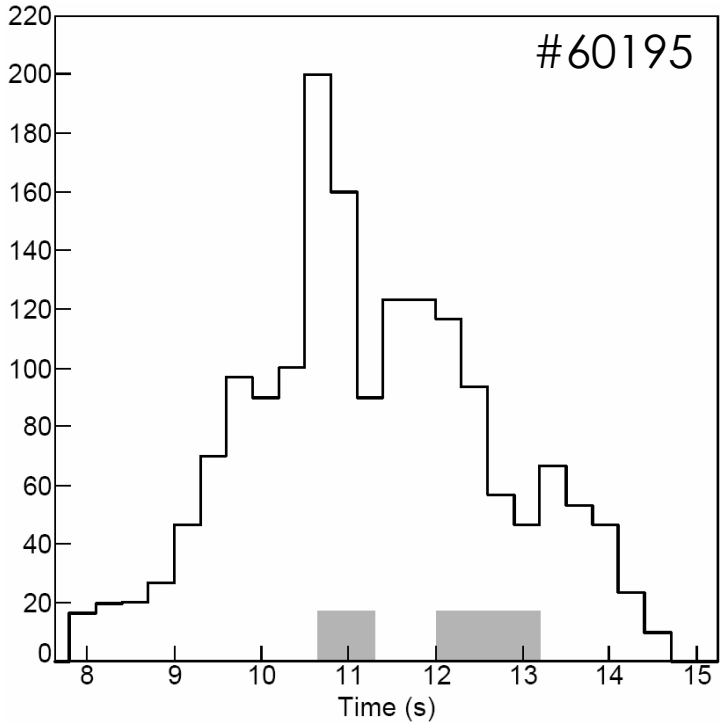

Figure 1: Intensity of γ-rays born as a result of nuclear inelastic scattering between ICRF accelerated minority hydrogen ions and carbon. The measurements are made with the vertical γ-ray spectrometer on JET and the grey time intervals indicate the periods when core-localised TAE activity is observed. Note that this is coincident with a significant decrease in the γ-ray intensity observed.

In order to calculate the distribution of fast ions produced by the minority hydrogen ICRF heating scheme used in the experiments referred to above (5.5 MW of couple power at 42 MHz and +90 phasing) simulations were performed using the PION code [9]. These indicated a perpendicular tail temperature that decreased approximately exponentially with increasing minor radius, ($f_E \sim \exp(-E/T)$ where $T \sim \exp(-r/L_T)$ and $L_T = 0.2$), with a temperature of approximately 500 keV at half the minor radius.

Combining the cross-section data for the production of γ-rays from the $^{12}C(p,p'\gamma)^{12}C$ reaction with the energy distribution of the ICRF heated fast ions as calculated by the PION code results in a narrow energy window over which the fast ions can be observed via γ-ray imaging of this spectral line as shown in Figure 2. Indeed, it is therefore protons with an energy around 5 MeV that are observed to be re-distributed or lost by the γ-ray data.

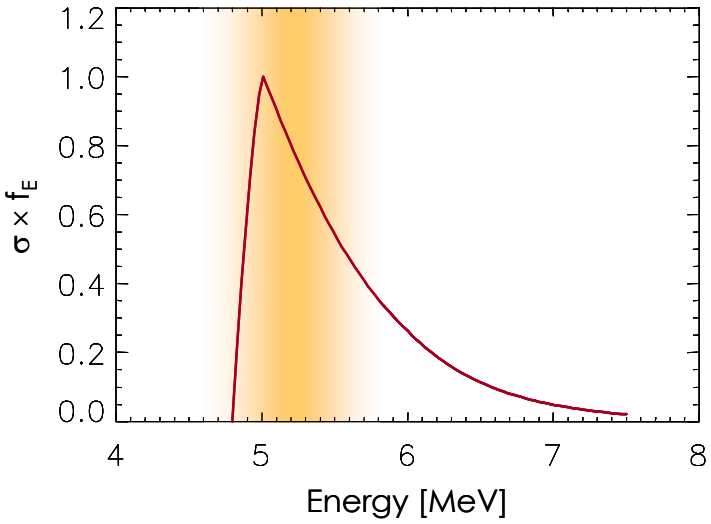

Figure 2: Cross-section, σ, for creation of γ–rays via nuclear inelastic scattering between energetic protons and ^{12}C combined with PION calculated ICRF ion distribution, f_E. The shaded region indicates the range of proton energies from which the majority of γ-rays are produced.

Turning to the modes responsible for the change in fast ion distribution, the core-localised TAE, or "tornado modes", one sees from Figure 3 showing a spectrogram (sliding Fourier transform) of the measurements made with a fast magnetic probe at the periphery of the plasma, that many discrete modes are present and that they sweep in frequency by around 15%. Note also that at around t = 13.05 s the observed Alfvénic activity is terminated by the occurrence of a monster sawtooth crash which may have been triggered by the loss of fast ion stabilisation [10,11,12].

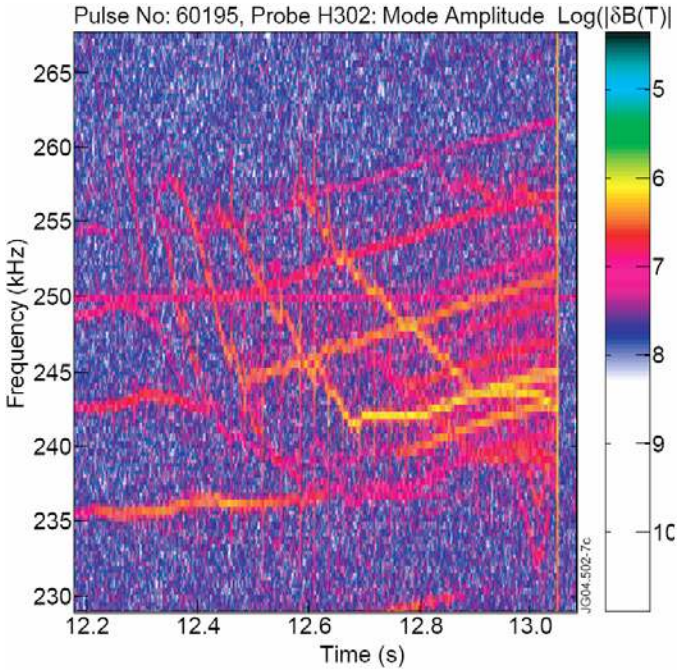

Figure 3: Spectrogram showing core localised TAE activity within the q = 1 surface ("tornado modes"). During this time interval the gamma-ray emmssion more than halves indicating a strong reduction in the number of 5 MeV protons in the plasma. At t = 13.05 s a monster sawtooth crash terminates the observed Alfvénic activity.

Starting from a detailed equilibrium reconstruction for this case (JET #60195 at t = 13s), calculations with the CASTOR code [13] were performed to obtain the linear MHD eigenfunctions of the n = 3 – 7 core-localised TAE observed. The results of these calculations are presented in Figure 4.

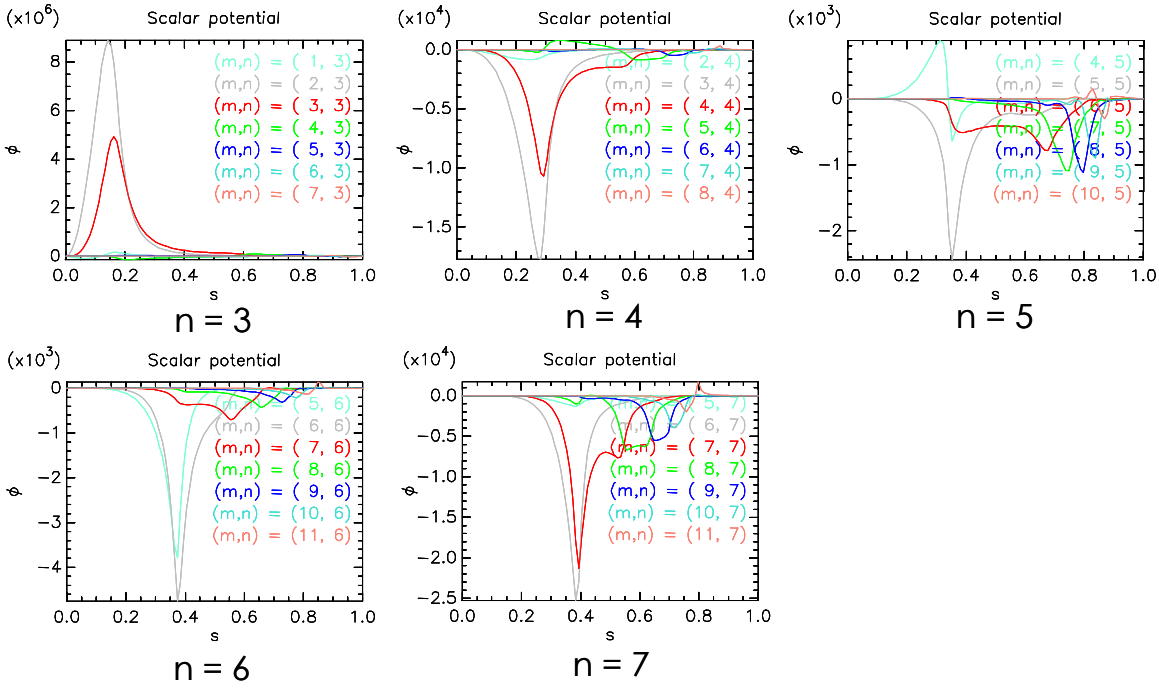

Figure 4: Linear MHD eigenfunctions of n = 3 – 7 core localised TAE (tornado modes) calculated with the CASTOR code for JET #60195 at t = 13s.

The frequency of the ion cyclotron resonance heating (ICRH) scheme used was chosen to heat the minority hydrogen ions at the radius of the magnetic axis. This created a distribution of trapped high-energy (E > 5MeV) protons, examples of which are shown in Figure 5.

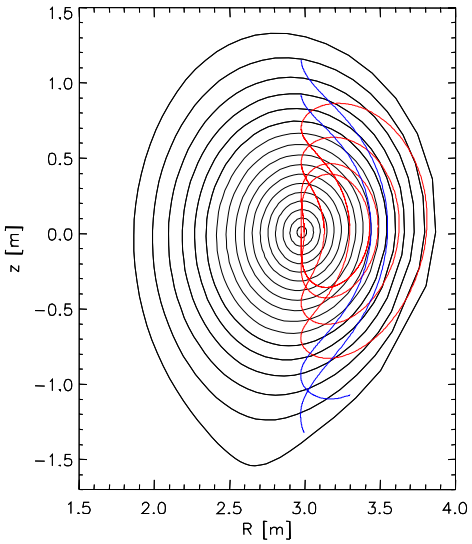

Figure 5: Guiding centre trajectories calculated with the HAGIS code of 5 MeV protons accelerated by on-axis ICRH in JET #60195 (I_p = 2 MA, B_t = 2.7 T). Note how deep within the plasma the turning points of the trapped ions must be for them to remain confined.

The properties of these orbits have been investigated using the HAGIS code [14] where the class of fast ions considered was described by the orbit invariant $\Lambda = \mu B_0 / E = 1$. This corresponds to trapped orbits with turning points at the on-axis ICRH resonance layer. The toroidal precession frequencies, ω_ϕ, and the poloidal transit frequencies, ω_θ, of this class of particles are presented in Figure 6 and Figure 7 respectively, where the toroidal precession frequency was calculated by the expression, $\omega_\phi = \langle \dot{\phi} \rangle = \oint \dot{\phi} dt \Big/ \oint dt = \Delta\phi / \Delta t$, and the integral is around a single closed poloidal orbit projection. For the poloidal orbit frequency the equivalent integral expression reduces to $\omega_\theta = 2\pi / \Delta t$.

The choice of z (height of turning point above mid-plane) as the orbit invariant to use in these plots as the ordinate was made to highlight the large extend of the prompt loss region which is itself a consequence of the large orbit widths of these trapped ions. For the ions of particular interest (i.e. those contributing most to the observed γ-rays), $E \sim 5$ MeV, those with turning points in the outer 25% of the minor radius are not on confined orbits and constitute prompt loss particles. At higher energies, this loss region is even larger with the outer 40% of the minor radius being on prompt loss trajectories at $E \sim 7$ MeV. The use of z as the phase-space variable in these plots is entirely equivalent to the more conventional use of P_ϕ (toroidal canonical momentum) in this (special) case since at the turning points, $P_\phi = \psi_p(z)$ where ψ_p is the poloidal flux and it should be recalled that it was an on-axis ICRF heating scheme that was used, so the turning points all line on a $|B|$ contour passing vertically through the magnetic axis.

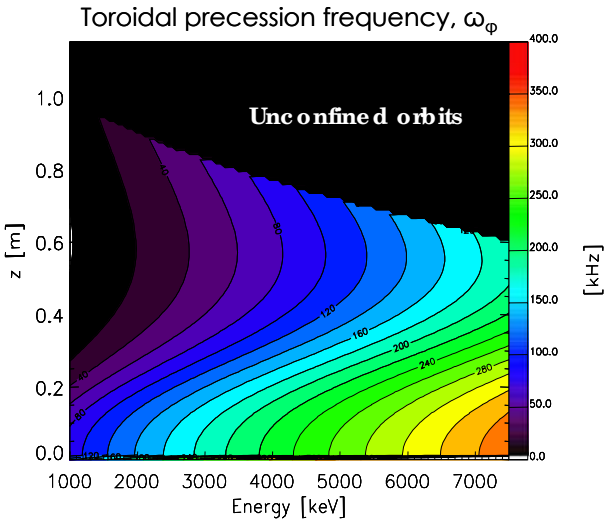

Figure 6: Toroidal precession frequency of protons with on-axis turning points described by $\Lambda = \mu B_0 / E = 1$. The vertical axis corresponds to the height of the turning points, $z(P_\phi)$, above the midplane.

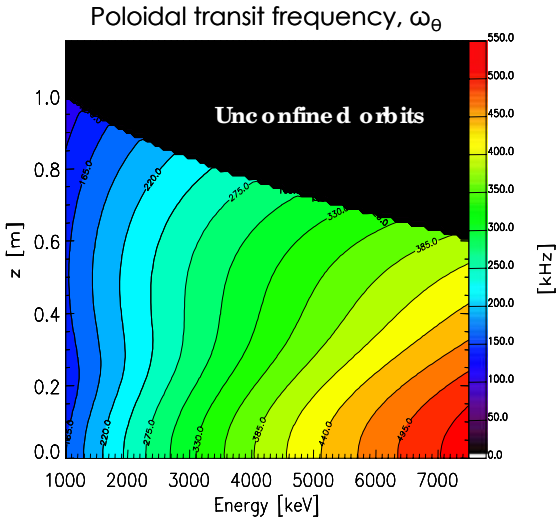

Figure 7: Poloidal transit frequency of protons with on-axis turning points described by $\Lambda = \mu B_0 / E = 1$. The vertical axis corresponds to the height of the turning point, $z(P_\phi)$, above the midplane.

The resonance condition for energetic ions to interact with a wave-field is $\Omega_{np} = n\omega_\phi - p\omega_\theta - \omega = 0$, where n is the toroidal wave number, p is the bounce harmonic and ω is the wave frequency. By plotting $1/\Omega_{np}$ for the range of particles investigated it is possible to identify the regions of phase-space where a resonant interaction could occur, as shown in Figure 8.

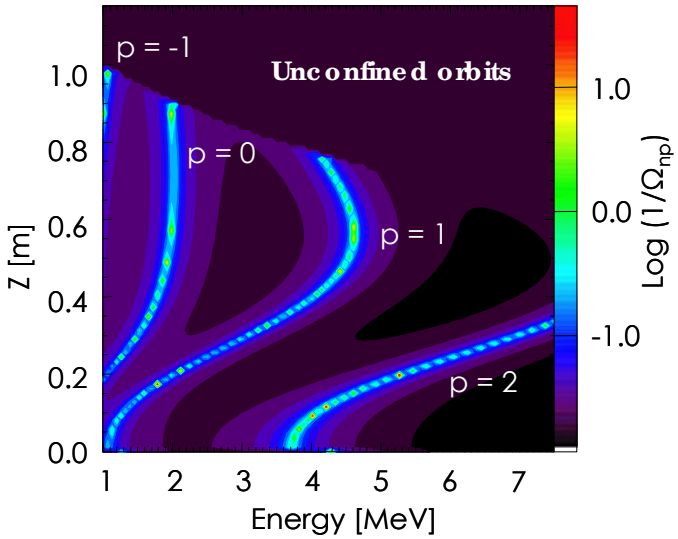

Figure 8: On-axis ICRH heated hydrogen ions that can resonant with the n = 3 low-shear TAE. The p values shown in the figure indicate the bounce harmonics involved in a particular phase-space resonance.

By combining the information regarding which ions contribute to the observed γ-ray emissions (Figure 2) with that depicting where the lines of resonances in phase-space are, such as shown in Figure 8, it is possible to indicate which resonances play a role in the observed decrease in γ-ray emission. This is done in Figure 9 where now the phase-space plotted is the more conventional E,P_ϕ space. Through their interaction with the waves, the particles move along straight lines described by $E-(\omega/n)P_\phi = K$, for some constant K. Since TAE are low frequency waves (compared with the cyclotron frequency) this interaction results in a predominant exchange of toroidal angular canonical moment, P_ϕ, which at the tips of the orbits where the parallel velocity is zero translates directly into a radial movement of the banana tips. This effect is also indicated in this figure through the over-plotting of the fine white lines. The "width" of the resonances is related to the nonlinear bounce frequency of the ions trapped in the potential well of the wave-field. The fact that the interaction of the fast protons with the core-localised TAE leads to a predominant change in radius (equivalent to change in P_ϕ), rules out an extensive re-distribution of fast ions in energy being responsible for the observed reduction in γ-ray emissions seen in JET: the modes are simply incapable of leading to a significant enough re-distribution in energy.

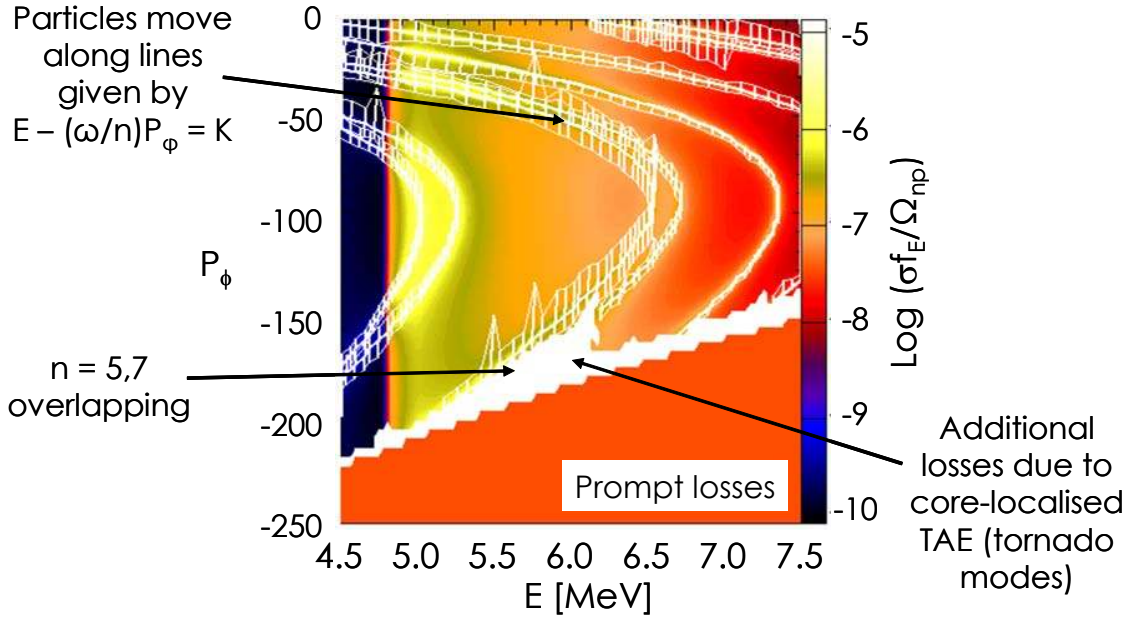

Figure 9: Resonance lines and motion of fast ions in phase-space due to the interaction with each of the core-localised TAE (n = 3 – 7) present in JET #60195. The amplitudes of the modes in these simulations was $\delta B/B = 10^{-2}$. An increase in the prompt loss region due to the presence of the modes is clearly visible, especially in the region where the n=5, p=2 and n=7, p=3 resonances overlap.

Despite there being a resonance at around 5 MeV, i.e. the region that produces the strongest γ-ray emission, the region of most enhanced loss (over and above the prompt losses) occurs at a slightly higher energy and arises due to the overlap of the n=5, p=2 and n=7, p=3 resonances. Recalling experimentally that the frequencies of the modes sweep by ~15%, it is found that this overlap region also sweeps and can therefore lead to losses over a large range of energies including those that contribute most significantly (E ~ 5 MeV) to the

generation of γ-rays through nuclear inelastic scattering with the carbon impurities present in the plasma. The results of such a 15% sweep in frequency are presented in Figure 10 which depicts the effect upon the position of the phase-space resonances through a decrease in frequency of 15% in 3% steps. (For clarity, the motion of the resonant ions is omitted in this figure when compared with Figure 9.)

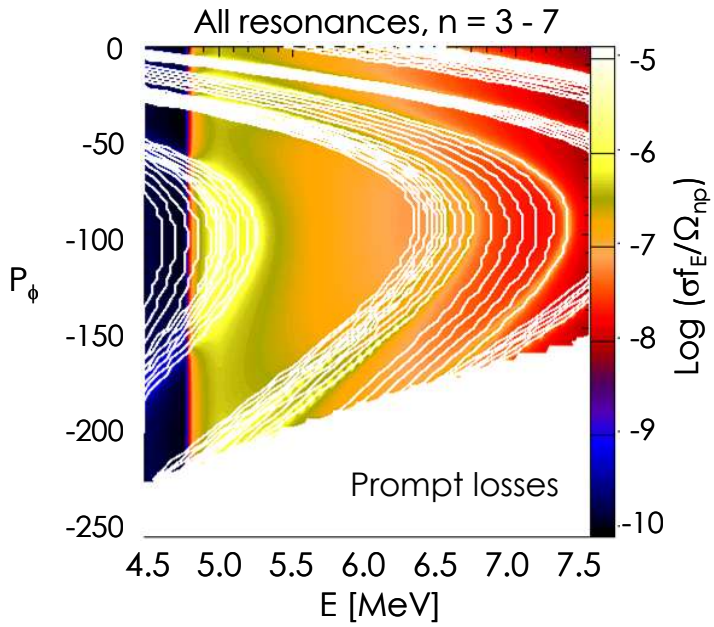

Figure 10: Movement of n = 3 – 7 core-localised TAE phase-space resonances that arises from sweeping the mode frequencies down in 3% steps over 15%.

In this case, the overlapping resonance lines sweep along the whole edge of the prompt loss boundary and can be expected to lead to losses over a wide range of energies, including that accountable for the observed decrease in the γ-ray emissivity of the plasma. We thus conclude that the observed dramatic drop in γ-ray emission during "tornado mode" activity seen on JET is due to the loss of 5 MeV protons arising from the phase-space overlap of the core-localised TAE resonances and not from a re-distribution of the fast protons in energy out of the region predominantly responsible for the observed γ-rays.

A quantitative comparison of the losses observed with a nonlinear simulation of the evolution of the fast ions and AE present using the HAGIS code [14] will form the basis of a future publication.

In the following two sections, the new diagnostic capabilities of ASDEX Upgrade and JET in the field of fast ion loss measurements is discussed.

New Fast Ion Loss Detector on ASDEX Upgrade

The new fast ion loss detector on ASDEX Upgrade [15] is installed on the mid-plane manipulator allowing the radial location of the detector to be optimised depending on the phenomena under investigation. The system is based upon the emission of light when collimated charged particles strike a scintillating material and the design used allows ions with energies between 5 keV and 160 keV and pitch angles, $\lambda = v_{\|}/v$, in the range

$0.14 < \lambda < 0.92$, i.e. deeply trapped to passing, to be detected. Compared to previous similar detectors, the scintillator used has a very fast decay time (<1μs) allowing very fast loss events to be resolved. The light emitted by the fast ions striking the scintillator plate is recorded using a high spatial resolution CCD camera with a moderate frame rate of between 25 and 100 Hz and in parallel, via a beam splitter arrangement and fibre optic bundle, a set of photomultipliers. The latter detectors can sample at up to 1MHz over a pre-selected array of fields on the scintillator plate enabling very fast events to be recorded at a reduced energy/pitch angle resolution.

Losses due to ELMs and NTMs have already been reported using this new system [15,16] and in Figure 11 the stochastic, multiple burst nature of losses observed during ELMs is shown.

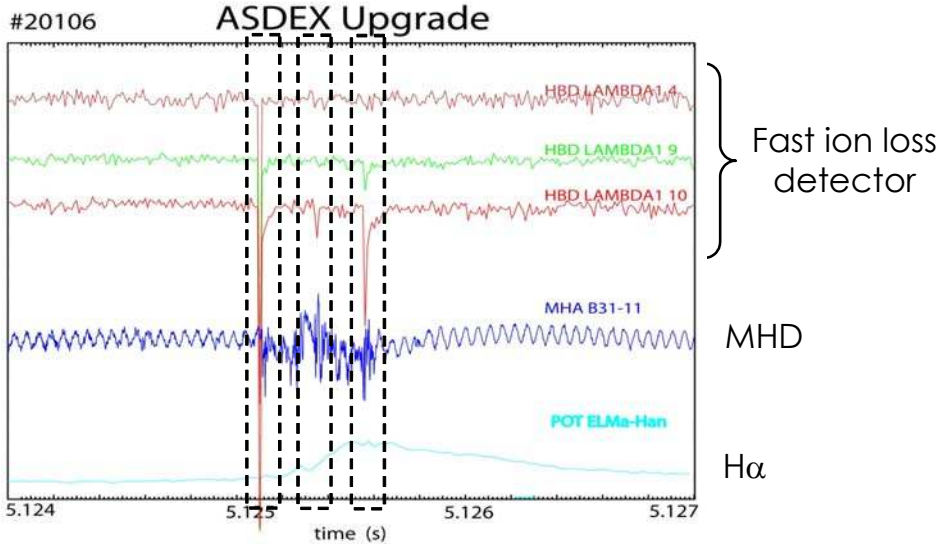

Figure 11: Observation of fast ion losses within a single ELM burst. The top three time traces correspond to photomultiplier channels showing losses corresponding to E = pitch=, etc. The next trace show the MHD activity detected by a magnetic coil at the edge of the plasma and the bottom line the H_α light emitted from the edge of the plasma during the ELM event.

Fast ion losses arising from the presence of neoclassical tearing modes (NTMs) have also been observed. For 3/2 NTMs the losses are correlated with the ELM activity whilst for 2/1 NTMs a resonance condition appears to have to be fulfilled before losses are observed: only once the island rotation has slowed to around 2.5 kHz are significant losses observed. In this case, the losses are not correlated with the ELMs but rather with the motion of the magnetic island structure past the detector head.

Localised losses in velocity-space in phase with the wave have also been observed during TAE activity and interpreted as direct evidence of a wave-particle resonance. These results will be reported elsewhere.

New Lost Alpha Detectors on JET

Two new enhancement projects to implement new fast ion loss detectors in JET are presently nearing completion. One of the systems is based around a Faraday cup array [3] and the other around a scintillator system [2]. The former system aims at providing

information on the energy and spatial distribution of the lost ions (5 poloidal and 3 radial detectors on the low field side) with a good time resolution (1 ms sampling time). The latter scintillator system makes a local measurement (also on the low field side) of the fast ion losses, resolving the pitch angle to within 5% and the gyro-radius to within 15%. The mapping of pitch angles and gyro-radii onto the scintillator plate was done using a 3D Monte-Carlo code that integrates the full equations of motion for individual ions taking into account the actual magnetic field of JET. The scientific exploitation of these detectors is planned to start in 2006.

In connection with these diagnostic enhancements, the consequence of toroidal field ripple is an area that JET plans to investigate further in future dedicated ripple experiments. By operating half of JET's 32 toroidal field coils at a slightly different current from the other half, the ripple magnitude can be varied and the detailed consequences on, amongst other phenomena, fast ion confinement investigated.

Controlled experiments investigating the influence of toroidal field ripple on the confinement of fast ions in the range from ~100 keV to ~3MeV were first performed in JET in the early 1990s [13]. Using only 16 out of the 32 TF coils available resulted in an increase of the ripple, which had a detrimental effect on the plasma behaviour. Comparing 16 coil discharges with 32 coil reference discharges led to a reduction in the total stored plasma energy of NBI heated L-mode plasmas by ~30% and a reduction of the ion heating. Thus, these experiments demonstrated how the confinement of energetic particles is degraded in the presence of a toroidal field ripple.

Summary and Conclusions

Studies of the cause for the substantial reduction in the γ-ray emission from JET plasmas exhibiting core-localised TAE mode activity within the q=1 surface ("tornado modes") indicate that the resonant overlap of neighbouring resonances close to the prompt loss boundary is responsible. For the particular case investigated, JET #60195, the sweep in frequency of the overlapping n = 5 and n = 7 TAE present ensured that the energy at which enhanced losses occurred aligned with the region of phase-space that contributed most significantly to the observed γ-rays production.

New fast ion loss detectors have recently been installed on both JET and ASDEX Upgrade. The JET diagnostics are expected to become operational this year whilst the first observations from ASDEX Upgrade already promise a rich programme of research on the physics of fast ion loss.

Future work will focus upon integrating the improved diagnostic capabilities that will soon become available with more extensive nonlinear simulations of the wave-particle interaction.

References

[1] S. D. Pinches *et al.*, Plasma Phys. Control. Fus. **46** (2004) B187
[2] S. Bäumel *et al.*, Rev. Sci. Instrum. **75** (2004) 3563
[3] D. S. Darrow *et al.*, Rev. Sci. Instrum. **75** (2004) 3566
[4] R. G. Goldston, R. B. White and A. H. Boozer, Phys. Rev. Lett. **47** (1981) 647–8
[5] H. L. Berk *et al.,* Phys. Plasmas **2** (1995) 3401

[6] G. J. Kramer *et al.,* Phys. Rev. Lett. **92** (2004) 015001
[7] V.G. Kiptily, Nuclear Fusion **42** (2002) 999
[8] S. E. Sharapov *et al.*, Nuclear Fusion **45** (2005) 1168
[9] L-G. Eriksson, T. Hellsten and U. Willén, Nucl. Fusion **33** (1993) 1037
[10] W.W. Heidbrink *et al.,* Nuclear Fusion **39** (1999) 1369
[11] S. Bernabei *et al.,* Nuclear Fusion **41** (2001) 513
[12] S. Bernabei *et al.,* Phys. Rev. Lett. **84** (2000) 1212
]13] W. Kerner *et al.,* J. Comput. Phys. **142** (1998) 271
[14] S. D. Pinches *et al.*, Comput. Phys. Comm. **111** (1998) 131
[15] M. García-Muñoz *et al.*, 32nd EPS Plasma Physics Conference, Tarragona, Spain (2005) P5.085
[16] M. García-Muñoz *et al.*, Submitted to Phys. Rev. Lett. (2005)